

Subset selection for linear mixed models

Daniel R. Kowal*

July 28, 2021

Abstract

Linear mixed models (LMMs) are instrumental for regression analysis with structured dependence, such as grouped, clustered, or multilevel data. However, selection among the covariates—while accounting for this structured dependence—remains a challenge. We introduce a Bayesian decision analysis for subset selection with LMMs. Using a Mahalanobis loss function that incorporates the structured dependence, we derive optimal linear actions for any subset of covariates and under any Bayesian LMM. Crucially, these actions inherit shrinkage or regularization and uncertainty quantification from the underlying Bayesian LMM. Rather than selecting a single “best” subset, which is often unstable and limited in its information content, we collect the *acceptable family* of subsets that nearly match the predictive ability of the “best” subset. The acceptable family is summarized by its smallest member and key variable importance metrics. Customized subset search and out-of-sample approximation algorithms are provided for more scalable computing. These tools are applied to simulated data and a longitudinal physical activity dataset, and in both cases demonstrate excellent prediction, estimation, and selection ability.

Keywords: Bayesian analysis; hierarchical models; prediction; regression; variable selection

*Dobelman Family Assistant Professor, Department of Statistics, Rice University, Houston, TX (daniel.kowal@rice.edu).

1 Introduction

Linear mixed models (LMMs) enable regression analysis in the presence of structured dependence, such as longitudinal data, grouped or clustered observations, or spatio-temporal effects. LMMs are widespread in both Bayesian and classical statistical analysis and include many hierarchical models and linear regression as special cases. We consider LMMs of the general form

$$\mathbf{y} = \mathbf{X}\boldsymbol{\beta} + \mathbf{Z}\mathbf{u} + \boldsymbol{\epsilon}, \tag{1}$$

where \mathbf{y} is the N -dimensional response, \mathbf{X} is the $N \times p$ matrix of covariates, $\boldsymbol{\beta}$ is the p -dimensional vector of fixed effects regression coefficients, \mathbf{Z} is the $N \times q$ random effects design matrix, \mathbf{u} is the q -dimensional vector of random effects regression coefficients, and $\boldsymbol{\epsilon}$ is the N -dimensional observation error. Model (1) is paired with the assumptions that \mathbf{u} and $\boldsymbol{\epsilon}$ are uncorrelated and mean zero with $\text{Cov}(\mathbf{u}) = \boldsymbol{\Sigma}_u$ and $\text{Cov}(\boldsymbol{\epsilon}) = \boldsymbol{\Sigma}_\epsilon$. Most commonly, the random effects \mathbf{u} and the errors $\boldsymbol{\epsilon}$ are endowed with Gaussian distributions, but our approach does not require these distributional assumptions.

The benefit of the LMM (1) is that it marries the classical linear regression term $\mathbf{X}\boldsymbol{\beta}$ with a random effects term $\mathbf{Z}\mathbf{u}$ to capture structural dependence unexplained by $\mathbf{X}\boldsymbol{\beta}$. More formally, (1) can be expressed in marginal form:

$$\mathbf{y} = \mathbf{X}\boldsymbol{\beta} + \boldsymbol{\nu} \tag{2}$$

where $\boldsymbol{\nu} := \mathbf{Z}\mathbf{u} + \boldsymbol{\epsilon}$ has mean zero and covariance $\mathbf{Z}\boldsymbol{\Sigma}_u\mathbf{Z}' + \boldsymbol{\Sigma}_\epsilon$. The covariance of $\boldsymbol{\nu}$ incorporates elements of the random effects design \mathbf{Z} , the random effects covariance $\boldsymbol{\Sigma}_u$, and the observation error covariance $\boldsymbol{\Sigma}_\epsilon$. As a result, LMMs are capable of modeling a broad variety of dependence structures; specific examples are given in Section 2.1.

Regardless of the structured dependence in the LMM, a core goal of regression analysis is

selection among the p (fixed effects) covariates \mathbf{x} . Selection provides interpretable summaries of the data, reduced storage requirement, and often better prediction and lower estimation variability. We emphasize four main priorities that motivate our approach:

- (P1) The selection criteria and accompanying performance metrics should account for the *structured dependence* modeled by the LMM;
- (P2) Selection should be applied *jointly* across covariates rather than *marginally* for each covariate;
- (P3) Selection of a *single* “best” subset of covariates should be replaced by a *collection* of “nearly-optimal” subsets of covariates; and
- (P4) The selection procedure should be computationally scalable in N and p .

P1 simply states that any structured dependence worth modeling in the LMM must also be incorporated into the selection and evaluation process—which renders many existing regression tools ineligible. P2 notes that variables selected using marginal criteria, such as hypothesis tests of the form $H_{0j} : \beta_j = 0$ or posterior inclusion probabilities from sparse Bayesian models, do not necessarily satisfy any joint optimality criteria. Hence, reporting the marginally-selected covariates as a joint subset of covariates often lacks justification. More directly, P2 is satisfied only for subset selection. Yet subset selection is accompanied by other challenges, most notably selection instability and computational scalability. P3 addresses the instability of subset selection: the “best” subset often changes dramatically under minor perturbations or resampling of the data. This effect is most pronounced in the presence of correlated covariates, weak signals, or small sample sizes, and undermines the elevated status of a “best” subset. By instead collecting “nearly-optimal” subsets, we acquire more information about the competing (predictive) explanations. Lastly, P4 recognizes the computational burdens of subset search and demands tools that are feasible for moderate to large N and p .

Variable selection for LMMs has most commonly relied on penalized maximum likelihood estimation. Foster et al. (2007) and Wang et al. (2011) incorporated random effects within an adaptive lasso estimation procedure to account for genetic and experimental effects in quantitative trait loci (QTL) analysis and plant population studies, respectively. Bondell et al. (2010) and Ibrahim et al. (2011) selected fixed and random effects jointly using a modified Cholesky decomposition with adaptive lasso or SCAD penalties. These Cholesky parametrizations are order-dependent, so permutations of the columns of \mathbf{Z} can produce different estimates and selections. Müller et al. (2013) also noted that the accompanying algorithms can be slow and fail to converge, and reviewed alternative strategies such as information criteria. Fan and Li (2012) selected fixed effects by marginalizing over the random effects and maximizing a penalized (marginal) log-likelihood. The primary limitation is the need for a “proxy matrix” for the inverse marginal covariance in (2); Fan and Li (2012) simply used a multiple of the identity matrix, but this ignores the random effects covariance structure. In general, such penalized estimators can address priorities P1, P2, and P4, but not P3: they focus on selecting a single “best” subset, and the accompanying (forward) search paths are too restrictive to enumerate a sufficiently rich collection of competitive subsets.

From a Bayesian perspective, Chen and Dunson (2003) and Kinney and Dunson (2007) proposed sparsity-inducing spike-and-slab priors for both the fixed and random effects. This choice of prior is entirely compatible with the proposed approach. The primary distinction is the mechanism for selection: Chen and Dunson (2003) and Kinney and Dunson (2007) compute posterior probabilities for all possible submodels. However, this strategy is computationally prohibitive and unreliable for small to moderate $p + q$, since only a small fraction of possible subsets can be visited regularly within the stochastic search Gibbs sampler. Hence, P4 is not satisfied. Marginal criteria such as posterior inclusion probabilities or hard-thresholding resolve these challenges, but fail to satisfy P2.

More broadly, Lindley (1968) and Hahn and Carvalho (2015) have argued that selection is a *decision problem* distinct from model specification. Sparsity or shrinkage priors cannot alone select variables: the prior is a component of the Bayesian model while the selection process requires its own criteria, typically a loss function that balances accuracy with sparsity. This decision analysis approach to selection has proven useful for functional regression (Kowal and Bourgeois, 2020), seemingly unrelated regressions (Puelz et al., 2017), and graphical models (Bashir et al., 2019), among others. However, these methods were not designed for LMMs and therefore fail to satisfy P1. In addition, with the exception of Kowal (2021a), these decision analysis approaches use (variations of) ℓ_1 -penalties and suffer from the same restrictive search paths as in classical penalized regression, which fails to satisfy P3.

We propose a Bayesian approach for subset search and selection in LMMs that satisfies P1–P4. Using decision analysis with a predictive loss function that directly incorporates the structured dependence in (1), we derive and compute the optimal linear actions (or estimators) for *any* subset $\mathcal{S} \subseteq \{1, \dots, p\}$ of covariates (P1, P2). These optimal actions are computable for any Bayesian LMM and inherit model-based regularization and posterior predictive uncertainty quantification. Linear actions are compared across subsets using out-of-sample predictive performance metrics that leverage both the structural dependence information and the predictive uncertainty from the Bayesian LMM. From these metrics, we construct the *acceptable family* of nearly-optimal subsets, which collects those subsets that perform nearly as well as the “best” subset with nonnegligible probability under the Bayesian LMM (P3). The acceptable family is more informative and robust than the “best” subset—which itself is a member—and is summarized using other key member subsets and variable importance metrics. Customized subset search and out-of-sample approximation algorithms are provided to enable scalable computing (P4).

We focus on subset selection of *fixed effects* covariates, but note that the distinction between fixed and random effects is less pertinent for Bayesian modeling. Unlike frequentist

LMMs that place a prior only on the random effects, Bayesian models require a prior on all parameters. Here, we consider “fixed effects” as those covariates designated for selection, while “random effects” capture the structured dependence unmodeled by the fixed effects. Although the random effects do not undergo formal selection in our decision analysis, the choice of prior, such as shrinkage or sparsity priors, can mitigate the impact of including potentially unimportant random effects.

The paper is outlined as follows: Section 2 develops the methodology and algorithms; Section 3 provides results for simulated data; Section 4 presents an application to physical activity data; Section 5 concludes. Online materials include a document detailing the out-of-sample approximation algorithm, additional simulation results, and additional results from the NHANES application; and R code to reproduce the simulation study and data analysis.

2 Methods

2.1 Predictive decision analysis for linear mixed models

Bayesian analysis of LMMs pairs the model (1) with suitable priors on $\boldsymbol{\beta}$ and \mathbf{u} and a distributional choice for $\boldsymbol{\epsilon}$ to determine the likelihood, which is typically Gaussian. Specific choices will depend on the formulation of (1) and are discussed subsequently; for now, we denote a generic Bayesian LMM by \mathcal{M} . The Bayesian model \mathcal{M} provides a (posterior) data-generating process via the posterior predictive distribution,

$$p_{\mathcal{M}}\{\tilde{\mathbf{y}}(\tilde{\mathbf{X}}, \tilde{\mathbf{Z}}) \mid \mathbf{y}\} = \int p_{\mathcal{M}}\{\tilde{\mathbf{y}}(\tilde{\mathbf{X}}, \tilde{\mathbf{Z}}) \mid \boldsymbol{\theta}\} p_{\mathcal{M}}(\boldsymbol{\theta} \mid \mathbf{y}) d\boldsymbol{\theta}, \quad (3)$$

where $\boldsymbol{\theta}$ denotes the model \mathcal{M} parameters including $\boldsymbol{\beta}$, \mathbf{u} , and any covariance parameters. The terms in the integrand are defined by the likelihood in (1) evaluated at the covariate values $\tilde{\mathbf{X}}$ and $\tilde{\mathbf{Z}}$ and the joint posterior distribution under \mathcal{M} . Informally, (3) describes the distribution of future or unobserved data $\tilde{\mathbf{y}}$ at the design matrices $\tilde{\mathbf{X}}$ and $\tilde{\mathbf{Z}}$ conditional on

the observed data \mathbf{y} and according to model \mathcal{M} . The choice of $\tilde{\mathbf{X}}$ and $\tilde{\mathbf{Z}}$ can target covariate values or subpopulations of interest and determines the type of predictive observations, such as predictions for a new group or new measurements on an existing group.

While the posterior predictive distribution formalizes the model-based uncertainty about unobserved data $\tilde{\mathbf{y}}(\tilde{\mathbf{X}}, \tilde{\mathbf{Z}})$, *predictive decision analysis* determines the actions—point or interval predictions or estimators, selection among hypotheses, etc.—that provide optimal data-driven decision-making under \mathcal{M} . Here, the goals are to (i) compute optimal linear actions (or estimates) for any given subset $\mathcal{S} \subseteq \{1, \dots, p\}$ of (fixed effects) predictors and (ii) evaluate and compare predictive performance among subsets—all while adhering to the priorities P1–P4. Predictive decision analysis requires a loss function of the form $\mathcal{L}\{\tilde{\mathbf{y}}(\tilde{\mathbf{X}}, \tilde{\mathbf{Z}}), \boldsymbol{\delta}\}$, which enumerates the cost of an action $\boldsymbol{\delta}$ when $\tilde{\mathbf{y}}(\tilde{\mathbf{X}}, \tilde{\mathbf{Z}})$ is realized. In accordance with P1 and P2, we deploy a Mahalanobis loss function

$$\mathcal{L}\{\tilde{\mathbf{y}}(\tilde{\mathbf{X}}, \tilde{\mathbf{Z}}), \boldsymbol{\delta}_{\mathcal{S}}; \boldsymbol{\psi}\} = \|\tilde{\mathbf{y}}(\tilde{\mathbf{X}}, \tilde{\mathbf{Z}}) - \tilde{\mathbf{X}}\boldsymbol{\delta}_{\mathcal{S}}\|_{\boldsymbol{\Omega}_{\boldsymbol{\psi}}}^2 \quad (4)$$

where $\boldsymbol{\delta}_{\mathcal{S}}$ is the p -dimensional linear action with zero coefficients for any index $j \notin \mathcal{S}$ and the norm $\|\mathbf{v}\|_{\boldsymbol{\Omega}_{\boldsymbol{\psi}}}^2 = \mathbf{v}'\boldsymbol{\Omega}_{\boldsymbol{\psi}}\mathbf{v}$ depends on a positive definite weighting matrix $\boldsymbol{\Omega}_{\boldsymbol{\psi}}$ that can depend on model \mathcal{M} parameters $\boldsymbol{\psi}$.

For LMMs, a natural choice of $\boldsymbol{\Omega}_{\boldsymbol{\psi}}$ is the inverse marginal covariance of $\boldsymbol{\nu}$,

$$\boldsymbol{\Omega}_{\boldsymbol{\psi}} = (\tilde{\mathbf{Z}}\boldsymbol{\Sigma}_{\mathbf{u}}\tilde{\mathbf{Z}}' + \boldsymbol{\Sigma}_{\epsilon})^{-1} \quad (5)$$

with $\boldsymbol{\psi} = (\boldsymbol{\Sigma}_{\mathbf{u}}, \boldsymbol{\Sigma}_{\epsilon})$. While the central quantity $\tilde{\mathbf{y}}(\tilde{\mathbf{X}}, \tilde{\mathbf{Z}}) - \tilde{\mathbf{X}}\boldsymbol{\delta}_{\mathcal{S}}$ in (4) explicitly measures the linear predictive ability of a subset \mathcal{S} of covariates $\tilde{\mathbf{X}}$, the choice of (5) incorporates weighting to account for the structured dependences that are unknown yet modeled by the random effects under \mathcal{M} . With (5), the Mahalanobis loss (4) resembles a multivariate Gaussian (negative) log-likelihood. However, this mathematical similarity should not be

confused with a distributional assumption: the Mahalanobis predictive loss (4) inherits a joint posterior predictive distribution $p_{\mathcal{M}}\{\tilde{\mathbf{y}}(\tilde{\mathbf{X}}, \tilde{\mathbf{Z}}), \boldsymbol{\psi} \mid \mathbf{y}\}$ under \mathcal{M} .

For any subset \mathcal{S} , optimal actions are obtained by minimizing the posterior expected loss under \mathcal{M} :

$$\hat{\boldsymbol{\delta}}_{\mathcal{S}} := \arg \min_{\boldsymbol{\delta}_{\mathcal{S}}} \mathbb{E}_{[\tilde{\mathbf{y}}, \boldsymbol{\psi} \mid \mathbf{y}]} \mathcal{L}\{\tilde{\mathbf{y}}(\tilde{\mathbf{X}}, \tilde{\mathbf{Z}}), \boldsymbol{\delta}_{\mathcal{S}}; \boldsymbol{\psi}\}, \quad (6)$$

which averages over the joint uncertainty in $\tilde{\mathbf{y}}(\tilde{\mathbf{X}}, \tilde{\mathbf{Z}})$ and $\boldsymbol{\psi}$ conditional on the data \mathbf{y} and according to the model \mathcal{M} . The solution to (6) is derived explicitly:

Lemma 1. *When $\mathbb{E}_{[\tilde{\mathbf{y}}, \boldsymbol{\psi} \mid \mathbf{y}]} \|\tilde{\mathbf{y}}(\tilde{\mathbf{X}}, \tilde{\mathbf{Z}})\|_{\Omega_{\boldsymbol{\psi}}}^2 < \infty$, the optimal action in (6) for any subset \mathcal{S} is given by the nonzero entries*

$$\hat{\boldsymbol{\delta}}_{\mathcal{S}} = (\tilde{\mathbf{X}}'_{\mathcal{S}} \hat{\boldsymbol{\Omega}} \tilde{\mathbf{X}}_{\mathcal{S}})^{-1} \tilde{\mathbf{X}}'_{\mathcal{S}} \hat{\mathbf{y}}^{\Omega} \quad (7)$$

with zeros for indices $j \notin \mathcal{S}$, where $\tilde{\mathbf{X}}_{\mathcal{S}}$ subsets the columns of $\tilde{\mathbf{X}}$ based on \mathcal{S} and $\hat{\boldsymbol{\Omega}} := \mathbb{E}_{[\boldsymbol{\psi} \mid \mathbf{y}]} \boldsymbol{\Omega}_{\boldsymbol{\psi}}$ and $\hat{\mathbf{y}}^{\Omega} := \mathbb{E}_{[\tilde{\mathbf{y}}, \boldsymbol{\psi} \mid \mathbf{y}]} \{\boldsymbol{\Omega}_{\boldsymbol{\psi}} \tilde{\mathbf{y}}(\tilde{\mathbf{X}}, \tilde{\mathbf{Z}})\}$ are posterior expectations under \mathcal{M} .

Proof. The Mahalanobis predictive loss is expandable as $\mathcal{L}\{\tilde{\mathbf{y}}(\tilde{\mathbf{X}}, \tilde{\mathbf{Z}}), \boldsymbol{\delta}_{\mathcal{S}}; \boldsymbol{\psi}\} = \|\tilde{\mathbf{y}}(\tilde{\mathbf{X}}, \tilde{\mathbf{Z}})\|_{\Omega_{\boldsymbol{\psi}}}^2 + \boldsymbol{\delta}'_{\mathcal{S}} \tilde{\mathbf{X}}' \boldsymbol{\Omega}_{\boldsymbol{\psi}} \tilde{\mathbf{X}} \boldsymbol{\delta}_{\mathcal{S}} - 2\boldsymbol{\delta}'_{\mathcal{S}} \tilde{\mathbf{X}}' \boldsymbol{\Omega}_{\boldsymbol{\psi}} \tilde{\mathbf{y}}(\tilde{\mathbf{X}}, \tilde{\mathbf{Z}})$. Computing posterior expectations, the first term is finite (by assumption) and does not depend on $\boldsymbol{\delta}_{\mathcal{S}}$, the second term is $\boldsymbol{\delta}'_{\mathcal{S}} \tilde{\mathbf{X}}' \hat{\boldsymbol{\Omega}} \tilde{\mathbf{X}} \boldsymbol{\delta}_{\mathcal{S}}$, and the third term is $-2\boldsymbol{\delta}'_{\mathcal{S}} \tilde{\mathbf{X}}' \hat{\mathbf{y}}^{\Omega}$. Minimizing the resulting quantity is equivalent to solving the weighted least squares problem with response $\hat{\mathbf{y}}^{\Omega}$, covariate matrix $\tilde{\mathbf{X}}_{\mathcal{S}}$, and weight matrix $\hat{\boldsymbol{\Omega}}$. \square

Lemma 1 explicitly derives the optimal Bayesian estimator under Mahalanobis loss for any subset \mathcal{S} . The solution in (7) may be nonunique, in which case a generalized inverse may be substituted. Crucially, the optimal action $\hat{\boldsymbol{\delta}}_{\mathcal{S}}$ is a “fit to the fit” from \mathcal{M} , and therefore inherits shrinkage or regularization from the Bayesian LMM. For illustration, consider a fixed and known weighting matrix $\boldsymbol{\Omega}$: the pseudo-response variable is $\hat{\mathbf{y}}^{\Omega} = \boldsymbol{\Omega} \hat{\mathbf{y}}$ where $\hat{\mathbf{y}} := \mathbb{E}_{[\tilde{\mathbf{y}} \mid \mathbf{y}]} \tilde{\mathbf{y}}(\tilde{\mathbf{X}}, \tilde{\mathbf{Z}}) = \tilde{\mathbf{X}} \hat{\boldsymbol{\beta}} + \tilde{\mathbf{Z}} \hat{\mathbf{u}}$ for $\hat{\boldsymbol{\beta}} := \mathbb{E}_{[\boldsymbol{\beta} \mid \mathbf{y}]} \boldsymbol{\beta}$ and $\hat{\mathbf{u}} := \mathbb{E}_{[\mathbf{u} \mid \mathbf{y}]} \mathbf{u}$. The regularization from \mathcal{M} —usually applied via the priors for $\boldsymbol{\beta}$ and \mathbf{u} —is valuable for point prediction and

estimation, and its absence in classical subset selection is detrimental (Hastie et al., 2020).

Remark. Lemma 1 does not require a LMM of the form (1): the results remain valid for the predictive variables $\tilde{\mathbf{y}}$ under any Bayesian model \mathcal{M} . The LMM guides our choice of $\mathbf{\Omega}_\psi$, but other options are available for different models \mathcal{M} . Similarly, Lemma 1 can be modified for *targeted prediction* (Kowal, 2021b) by substituting $h\{\tilde{\mathbf{y}}(\tilde{\mathbf{X}}, \tilde{\mathbf{Z}})\}$ as the predictive variable, where h denotes the target functional of interest, and suitably modifying $\mathbf{\Omega}_\psi$.

The optimal action (7) resembles generalized least squares (GLS) estimation for linear regression, including LMMs. The primary challenge in GLS estimation is that the inverse covariance or weight matrix $\mathbf{\Omega}_\psi$ is unknown. Feasible GLS iteratively estimates the covariance and the linear coefficients via plug-in estimation, which is suboptimal. For LMMs, Fan and Li (2012) substituted a multiple of the identity matrix for $\mathbf{\Sigma}_u$ in (5) in order to avoid estimation of this covariance. These concessions are avoided in our approach: we solve a GLS optimization problem, but compute model-based expectations jointly over the unknown parameters—including the necessary inverse covariance matrix. The estimate of $\mathbf{\Omega}_\psi$ derives from the Bayesian LMM (1), which can benefit from the model-based regularization induced by the choice of shrinkage or sparsity priors under \mathcal{M} .

To illustrate the use of the weighting matrix $\mathbf{\Omega}_\psi$, we consider several examples. Since $\mathbf{\Omega}_\psi = \mathbf{\Sigma}_\epsilon^{-1} - \mathbf{\Sigma}_\epsilon^{-1} \tilde{\mathbf{Z}}(\mathbf{\Sigma}_u^{-1} + \tilde{\mathbf{Z}}' \mathbf{\Sigma}_\epsilon^{-1} \tilde{\mathbf{Z}})^{-1} \tilde{\mathbf{Z}}' \mathbf{\Sigma}_\epsilon^{-1}$ by the Woodbury identity, the common assumption of $\mathbf{\Sigma}_\epsilon = \sigma_\epsilon^2 \mathbf{I}_N$ results in the simplification

$$\mathbf{\Omega}_\psi = \sigma_\epsilon^{-2}(\mathbf{I}_N - \tilde{\mathbf{Z}} \mathbf{\Sigma}_{u^*}^{-1} \tilde{\mathbf{Z}}'), \quad (8)$$

where $\mathbf{\Sigma}_{u^*} := \sigma_\epsilon^2 \mathbf{\Sigma}_u^{-1} + \tilde{\mathbf{Z}}' \tilde{\mathbf{Z}}$. The Mahalanobis predictive loss (4) then decomposes as

$$\sigma_\epsilon^2 \mathcal{L}\{\tilde{\mathbf{y}}(\tilde{\mathbf{X}}, \tilde{\mathbf{Z}}), \delta_S; \psi\} = \|\tilde{\mathbf{y}}(\tilde{\mathbf{X}}, \tilde{\mathbf{Z}}) - \tilde{\mathbf{X}} \delta_S\|_2^2 - \|\tilde{\mathbf{y}}(\tilde{\mathbf{X}}, \tilde{\mathbf{Z}}) - \tilde{\mathbf{X}} \delta_S\|_{\tilde{\mathbf{Z}} \mathbf{\Sigma}_{u^*}^{-1} \tilde{\mathbf{Z}}'}^2$$

which isolates the contribution from the squared error loss and the Mahalanobis loss based only on $\tilde{\mathbf{Z}}$ and $\Sigma_{\mathbf{u}^*}$ —i.e., the critical terms in the random effects component.

The optimal action (7) requires computation of $\hat{\Omega}$ and $\hat{\boldsymbol{\gamma}}^\Omega$ under \mathcal{M} . We further consider two important examples: the random intercept model (Section 2.1.1) and the random slope model (Section 2.1.2).

2.1.1 Random intercept model

Consider repeated or longitudinal observations $\{y_{ij}\}_{j=1}^{m_i}$ on each subject $i = 1, \dots, n$, so $N = \sum_{i=1}^n m_i$. The within-subject correlations are often modeled using the random intercept model

$$y_{ij} = \mathbf{x}'_i \boldsymbol{\beta} + u_i + \epsilon_{ij}, \quad (9)$$

usually with $u_i \stackrel{iid}{\sim} N(0, \sigma_u^2)$ and $\epsilon_{ij} \stackrel{iid}{\sim} N(0, \sigma_\epsilon^2)$, although normality is not required here. The crucial role of u_i cannot be ignored: σ_u accounts for the within-subject correlation, $\text{Corr}(y_{ij}, y_{ij'} \mid \mathbf{x}_i, \boldsymbol{\beta}) = \sigma_u^2 / (\sigma_u^2 + \sigma_\epsilon^2)$, that remains unexplained by the covariates \mathbf{x}_i . Model (9) is a special case of (1) with $\Sigma_{\mathbf{u}} = \sigma_u^2 \mathbf{I}_N$ and $\mathbf{Z} = \text{bdiag}\{\mathbf{1}_{m_i}\}_{i=1}^n$ is a block diagonal matrix composed of n m_i -dimensional vectors of ones.

For predictive decision analysis, let $\tilde{\mathbf{x}}_i$ denote the target covariate values and \tilde{m}_i the number of observations for each subject $i = 1, \dots, \tilde{n}$, which determines $\tilde{\mathbf{Z}}$. The subject-specific predictive variables are $\tilde{\boldsymbol{\gamma}}(\tilde{\mathbf{X}}, \tilde{\mathbf{Z}}) = (\tilde{\boldsymbol{\gamma}}'_1, \dots, \tilde{\boldsymbol{\gamma}}'_n)'$ with $\tilde{\boldsymbol{\gamma}}_i = (\tilde{y}_{i1}, \dots, \tilde{y}_{i\tilde{m}_i})'$ and the fixed effects covariate matrix is $\tilde{\mathbf{X}} = (\mathbf{1}'_{m_1} \otimes \tilde{\mathbf{x}}_1, \dots, \mathbf{1}'_{m_{\tilde{n}}} \otimes \tilde{\mathbf{x}}_{\tilde{n}})'$. To compute Ω_ψ , observe that $\Sigma_{\mathbf{u}^*} = \text{bdiag}\{\sigma_\epsilon^2 / \sigma_u^2 + \mathbf{1}'_{\tilde{m}_i} \mathbf{1}_{\tilde{m}_i}\}_{i=1}^n = \text{diag}\{\sigma_\epsilon^2 / \sigma_u^2 + \tilde{m}_i\}_{i=1}^n$ and $\Sigma_{\mathbf{u}^*}^{-1} = \text{diag}\{(\sigma_\epsilon^2 / \sigma_u^2 + \tilde{m}_i)^{-1}\}_{i=1}^n$, so the Mahalanobis weight matrix (up to σ_ϵ^2) is

$$\sigma_\epsilon^2 \Omega_\psi = \text{bdiag}\left\{ \mathbf{I}_{\tilde{m}_i} - \frac{1}{\sigma_\epsilon^2 / \sigma_u^2 + \tilde{m}_i} \mathbf{1}_{\tilde{m}_i} \mathbf{1}'_{\tilde{m}_i} \right\}_{i=1}^n \quad (10)$$

and does not require any numerical matrix inversions. Given (10), the Mahalanobis predictive

loss simplifies to

$$\sigma_\epsilon^2 \|\tilde{\mathbf{y}} - \tilde{\mathbf{X}} \boldsymbol{\delta}_S\|_{\Omega_\psi}^2 = \sum_{i=1}^{\tilde{n}} \left[\sum_{j=1}^{\tilde{m}_i} (\tilde{y}_{ij} - \tilde{\mathbf{x}}_i' \boldsymbol{\delta}_S)^2 - \frac{1}{\sigma_\epsilon^2 / \sigma_u^2 + \tilde{m}_i} \left\{ \sum_{j=1}^{\tilde{m}_i} (\tilde{y}_{ij} - \tilde{\mathbf{x}}_i' \boldsymbol{\delta}_S) \right\}^2 \right] \quad (11)$$

which clearly isolates the difference between the Mahalanobis loss and squared error loss. In particular, (11) incorporates the sign of the errors $e_{ij} := \tilde{y}_{ij} - \tilde{\mathbf{x}}_i' \boldsymbol{\delta}_S$. For example, suppose $\tilde{n} = 1$ and $\tilde{m}_1 = 2$, so the Mahalanobis loss (up to σ_ϵ^2) is $e_1^2 + e_2^2 - (\sigma_\epsilon^2 / \sigma_u^2 + 2)^{-1} (e_1 + e_2)^2$. The squared error loss $e_1^2 + e_2^2$ is invariant to the signs of the errors. However, the second term in (11) includes a reduction in the loss by a factor of $(e_1 + e_2)^2$, which is larger when the errors have the same sign. Compared to the squared error loss, this Mahalanobis loss is more forgiving for errors in the same direction—and this is accentuated when σ_u is large—which reflects the within-subject correlation induced by the underlying model (9).

The posterior expectation $\hat{\Omega}$ of (10) is straightforward to compute, for example given posterior samples of $\{\sigma_\epsilon^2, \sigma_u^2\}$. To compute the posterior expectation of $\Omega_\psi \tilde{\mathbf{y}}(\tilde{\mathbf{X}}, \tilde{\mathbf{Z}})$, the block diagonality simplifies this term to n blocks of the form $\sigma_\epsilon^{-2} \{\mathbf{I}_{\tilde{m}_i} - (\sigma_\epsilon^2 / \sigma_u^2 + \tilde{m}_i)^{-1} \mathbf{1}_{\tilde{m}_i} \mathbf{1}_{\tilde{m}_i}'\} \tilde{\mathbf{y}}_i = \sigma_\epsilon^{-2} \tilde{\mathbf{y}}_i - \{\sigma_\epsilon^{-2} (\sigma_\epsilon^2 / \sigma_u^2 + \tilde{m}_i)^{-1} \sum_{j=1}^{\tilde{m}_i} \tilde{y}_{ij}\} \mathbf{1}_{\tilde{m}_i}$. The posterior expectation of each \tilde{m}_i -dimensional vector is easily computable given posterior samples of $\{\sigma_\epsilon^2, \sigma_u^2, \tilde{\mathbf{y}}_i\}_{i=1}^{\tilde{n}}$.

2.1.2 Random slope model

Subject-specific slopes are common in hierarchical or multilevel models. By applying (1) with $\mathbf{Z} = \text{bdiag}\{\mathbf{x}'_i\}_{i=1}^n$, the random slope model allows for subject-specific deviations from the population-level coefficients $\boldsymbol{\beta}$:

$$y_i = \mathbf{x}'_i \boldsymbol{\beta}_i + \epsilon_i, \quad \boldsymbol{\beta}_i := \boldsymbol{\beta} + \mathbf{u}_i. \quad (12)$$

Model (12) is often accompanied by shrinkage priors on $\boldsymbol{\beta}$ and \mathbf{u}_i to regularize against unnecessary predictors and unnecessary heterogeneity, respectively. Predictive decision analysis

with Mahalanobis loss enables coefficient estimation and subset selection for \mathbf{x} (see Section 2.2) while adjusting for the heterogeneities induced by the random effects \mathbf{u}_i .

When $\Sigma_\epsilon = \sigma_\epsilon^2 \mathbf{I}_N$, the key term $\Sigma_{\mathbf{u}^*}^{-1}$ in the inverse covariance (8) is directly available from the Sherman-Morrison formula, $\Sigma_{\mathbf{u}^*}^{-1} = \sigma_\epsilon^{-2} \text{bdiag}\{\Sigma_{\mathbf{u}_i} - \Sigma_{\mathbf{u}_i} \tilde{\mathbf{x}}_i \tilde{\mathbf{x}}_i' \Sigma_{\mathbf{u}_i} / (\sigma_\epsilon^2 + \tilde{\mathbf{x}}_i' \Sigma_{\mathbf{u}_i} \tilde{\mathbf{x}}_i)\}_{i=1}^n$. The accompanying Mahalanobis weight matrix then simplifies to the diagonal matrix $\Omega_\psi = \text{diag}\{\omega_i\}_{i=1}^n$ with $\omega_i := 1/(\sigma_\epsilon^2 + \tilde{\mathbf{x}}_i' \Sigma_{\mathbf{u}_i} \tilde{\mathbf{x}}_i)$, which is computable without numerical matrix inversions. The implied Mahalanobis predictive loss is the weighted least squares $\|\tilde{\mathbf{y}}(\tilde{\mathbf{X}}, \tilde{\mathbf{Z}}) - \tilde{\mathbf{X}} \boldsymbol{\delta}_S\|_{\Omega_\psi}^2 = \sum_{i=1}^{\tilde{n}} \omega_i \{\tilde{y}_i(\tilde{\mathbf{x}}_i) - \tilde{\mathbf{x}}_i' \boldsymbol{\delta}_S\}^2$. The subject-specific weights ω_i are primarily driven by $\tilde{\mathbf{x}}_i' \Sigma_{\mathbf{u}_i} \tilde{\mathbf{x}}_i$, where $\Sigma_{\mathbf{u}_i}$ is the covariance of the subject-specific deviations $\mathbf{u}_i = \boldsymbol{\beta}_i - \boldsymbol{\beta}$. The posterior expectations required by Lemma 1 are straightforward: $\Omega_\psi = \text{diag}\{\omega_i\}_{i=1}^n$ and $\Omega_\psi \tilde{\mathbf{y}}(\tilde{\mathbf{X}}, \tilde{\mathbf{Z}})$ is an \tilde{n} -dimensional vector with elements $\{\omega_i \tilde{y}_i(\tilde{\mathbf{x}}_i)\}_{i=1}^{\tilde{n}}$, both of which are easily computable given posterior samples of $\{\sigma_\epsilon^2, \Sigma_{\mathbf{u}_i}, \tilde{y}_i(\tilde{\mathbf{x}}_i)\}_{i=1}^{\tilde{n}}$.

2.2 Acceptable families for nearly-optimal subsets

Although Lemma 1 produces optimal actions $\hat{\boldsymbol{\delta}}_S$ for a given subset S , it does not guide subset *selection*. Direct optimization over S is also unhelpful:

$$\hat{\boldsymbol{\delta}}_S := \arg \min_{S, \boldsymbol{\delta}_S} \mathbb{E}_{[\tilde{\mathbf{y}}, \psi | \mathbf{y}]} \mathcal{L}\{\tilde{\mathbf{y}}(\tilde{\mathbf{X}}, \tilde{\mathbf{Z}}), \boldsymbol{\delta}_S; \psi\} = \hat{\boldsymbol{\delta}}_{\{1, \dots, p\}} \quad (13)$$

trivially selects the full subset $\hat{S} = \{1, \dots, p\}$ with the coefficients from (7); the result is a consequence of Lemma 2 below. Hence, direct optimization cannot provide data-driven selection: the “optimal” subset is invariant to the data.

A popular decision analysis strategy for selection appends the loss function (e.g., (4)) with an ℓ_1 -penalty to encourage sparsity in $\boldsymbol{\delta}_{\{1, \dots, p\}}$ (Hahn and Carvalho, 2015). While this approach is compatible with our framework, we avoid it for two reasons. First, the ℓ_1 -penalty introduces additional regularization—beyond the regularization from \mathcal{M} —and can overshrink true signals. Adaptive lasso-type adjustments are available (Kowal et al., 2021)

but cannot circumvent this issue entirely. Second, the (adaptive) lasso-based search paths are highly constrained within the space of all possible subsets, and therefore cannot enumerate a sufficiently broad collection of competitive subsets to satisfy P3.

Instead, we collect the *acceptable family* of nearly-optimal subsets. Informally, the acceptable family is the collection of all subsets \mathcal{S} that match or nearly match the predictive performance of the “best” model with nonnegligible probability under \mathcal{M} . By studying this collection of nearly-optimal subsets, we deemphasize the role of a single “best” subset in favor of many distinct yet predictively-competitive alternatives. The acceptable family has been applied for Bayesian subset selection (Kowal, 2021a), ℓ_1 -penalized selection (Kowal et al., 2021), and targeted variable selection (Kowal, 2021b), but none of these cases consider LMMs or Mahalanobis loss.

The acceptable family is built by evaluating *out-of-sample* predictive performance, which requires careful consideration for LMMs. For repeated or longitudinal observations, it must be determined whether to evaluate predictions for new subjects or for new measurements on existing subjects. For concreteness, we proceed under the longitudinal setting of Section 2.1.1 and evaluate predictions on new subjects. However, modifications for other cases are available.

Specifically, suppose there are n subjects with m_i observations per subject, $i = 1, \dots, n$. We implement a Bayesian K -fold cross-validation procedure, where the K folds are taken across subjects $i = 1, \dots, n$. Let $\mathcal{I}_k \subset \{1, \dots, n\}$ denote the k th validation set, where each subject point appears in one validation set, $\cup_{k=1}^K \mathcal{I}_k = \{1, \dots, n\}$. By default, we use $K = 10$ validation sets that are equally-sized, mutually exclusive, and selected randomly from $\{1, \dots, n\}$. For each subset \mathcal{S} , we define the out-of-sample *empirical loss*

$$\mathcal{L}_{\mathcal{S}} := \frac{1}{K} \sum_{k=1}^K \mathcal{L}_{\mathcal{S}}(k), \quad \mathcal{L}_{\mathcal{S}}(k) := \frac{1}{|\mathcal{I}_k|} \mathcal{L}(\mathbf{y}_{\mathcal{I}_k}, \hat{\boldsymbol{\delta}}_{\mathcal{S}}^{-\mathcal{I}_k}; \hat{\boldsymbol{\psi}}^{-\mathcal{I}_k}), \quad (14)$$

where $\mathbf{y}_{\mathcal{I}_k} := \{\mathbf{y}_i\}_{i \in \mathcal{I}_k}$ denotes the response variables on the validation data with $\mathbf{y}_i = (y_{i1}, \dots, y_{im_i})'$, $\hat{\boldsymbol{\delta}}_{\mathcal{S}}^{-\mathcal{I}_k} := \arg \min_{\boldsymbol{\delta}_{\mathcal{S}}} \mathbb{E}_{[\tilde{\mathbf{y}}, \boldsymbol{\psi} | \mathbf{y}_{-\mathcal{I}_k}]} \mathcal{L}(\tilde{\mathbf{y}}_{\mathcal{I}_k}, \boldsymbol{\delta}_{\mathcal{S}}; \boldsymbol{\psi})$ is the optimal action (6) but estimated using only the training data $\mathbf{y}_{-\mathcal{I}_k} := \{\mathbf{y}_i\}_{i \notin \mathcal{I}_k}$, and, with abuse of notation, $\hat{\boldsymbol{\psi}}^{-\mathcal{I}_k}$ in (14) indicates the Mahalanobis loss (4) with weighting matrix $\hat{\boldsymbol{\Omega}}^{-\mathcal{I}_k} := \mathbb{E}_{[\boldsymbol{\psi} | \mathbf{y}_{-\mathcal{I}_k}]} \boldsymbol{\Omega}_{\boldsymbol{\psi}}$. The empirical loss (14) resembles classical K -fold cross-validation with a point estimate for each Mahalanobis loss weighting matrix. From this quantity, we define the “best” subset for out-of-sample point prediction,

$$\mathcal{S}_{min} := \arg \min_{\mathcal{S}} \mathcal{L}_{\mathcal{S}}, \quad (15)$$

so that $\hat{\boldsymbol{\delta}}_{\mathcal{S}_{min}}$ is the optimal linear action for the subset \mathcal{S}_{min} that minimizes (14).

To define the acceptable family, we first introduce the out-of-sample *predictive loss* analogous to (14):

$$\tilde{\mathcal{L}}_{\mathcal{S}} := \frac{1}{K} \sum_{k=1}^K \tilde{\mathcal{L}}_{\mathcal{S}}(k), \quad \tilde{\mathcal{L}}_{\mathcal{S}}(k) := \frac{1}{|\mathcal{I}_k|} \mathcal{L}(\tilde{\mathbf{y}}_{\mathcal{I}_k}^{-\mathcal{I}_k}, \hat{\boldsymbol{\delta}}_{\mathcal{S}}^{-\mathcal{I}_k}, \boldsymbol{\psi}^{-\mathcal{I}_k}) \quad (16)$$

where $\tilde{\mathbf{y}}_{\mathcal{I}_k}^{-\mathcal{I}_k} \sim p_{\mathcal{M}}[\{\tilde{\mathbf{y}}(\mathbf{x}_i, \mathbf{z}_i)\}_{i \in \mathcal{I}_k} | \mathbf{y}_{-\mathcal{I}_k}]$ denotes the predictive variables in the validation set conditional on the training data and $\boldsymbol{\psi}^{-\mathcal{I}_k}$ similarly conditions only on the training data. Unlike the empirical loss $\mathcal{L}_{\mathcal{S}}$, the predictive loss $\tilde{\mathcal{L}}_{\mathcal{S}}$ incorporates out-of-sample predictive *uncertainty* under \mathcal{M} , as well as the uncertainty regarding relevant model parameters $\boldsymbol{\psi}$. The uncertainty reflects the fact that the validation data $\mathbf{y}_{\mathcal{I}_k}$ represent only one possible realization of observables at the covariate values $\{\mathbf{x}_i, \mathbf{z}_i\}_{i \in \mathcal{I}_k}$. The (out-of-sample) predictive distribution provides alternative model-based realizations, and hence is informative for quantifying the uncertainty of out-of-sample predictive performance.

Using the predictive loss, the acceptable family is defined as those subsets that are “nearly-optimal” relative to \mathcal{S}_{min} :

$$\mathbb{A}_{\eta, \varepsilon} := \{\mathcal{S} : \mathbb{P}_{\mathcal{M}}(\tilde{\mathcal{D}}_{\mathcal{S}_{min}, \mathcal{S}} < \eta) \geq \varepsilon\}, \quad \eta \geq 0, \varepsilon \in [0, 1] \quad (17)$$

where $\tilde{\mathcal{D}}_{\mathcal{S}_{min},\mathcal{S}} := 100 \times (\tilde{\mathcal{L}}_{\mathcal{S}} - \tilde{\mathcal{L}}_{\mathcal{S}_{min}}) / \tilde{\mathcal{L}}_{\mathcal{S}_{min}}$ is the percent increase in predictive loss for subset \mathcal{S} relative to \mathcal{S}_{min} , $\eta \geq 0\%$ is the margin, and $\varepsilon \in [0, 1]$ is the probability level. Equivalently, a subset \mathcal{S} is acceptable if and only if there exists a lower $(1 - \varepsilon)$ posterior prediction interval for $\tilde{\mathcal{D}}_{\mathcal{S}_{min},\mathcal{S}}$ that includes η (Kowal, 2021b). Alternatively, subsets are *not* acceptable if there is insufficient predictive probability under \mathcal{M} that the out-of-sample accuracy is within a predetermined margin of the “best” subset. \mathcal{S}_{min} is necessarily a member of $\mathbb{A}_{\eta,\varepsilon}$ for any (η, ε) , so the acceptable family is always nonempty. Larger values of η and smaller values of ε expand the acceptable family; we select $\eta = 0$ and $\varepsilon = 0.10$ by default (see also Kowal, 2021b; Kowal et al., 2021; Kowal, 2021a for sensitivity evaluations).

The acceptable family is related to fence methods for model selection (Jiang et al., 2008), which seek to eliminate “incorrect” models using likelihood criteria. These methods rely on asymptotic arguments or bootstrap computations, while our approach emphasizes out-of-sample predictive performance with (finite-sample) predictive uncertainty quantification under the LMM. Moreover, fence methods focus on selection of a *single* model, rather than analysis of the *collection* of nearly-optimal models or subsets.

We summarize the acceptable family using two strategies. First, we report two key members: the “best” subset \mathcal{S}_{min} and the *smallest* acceptable subset,

$$\mathcal{S}_{small} := \arg \min_{\mathcal{S} \in \mathbb{A}_{\eta,\varepsilon}} |\mathcal{S}|, \quad (18)$$

which is the smallest subset of covariates that satisfies the near-optimality condition in (17). When \mathcal{S}_{small} is nonunique, we select from among those the subset with the smallest empirical loss (14). Typically, we find $|\mathcal{S}_{small}| \ll |\mathcal{S}_{min}|$ which is expected: selection based on minimizing cross-validation error is known to produce models that are unnecessarily complex.

Second, we summarize $\mathbb{A}_{\eta,\varepsilon}$ using the variable importance metric for each covariate j :

$$\text{VI}_{\text{incl}}(j) := |\mathbb{A}_{\eta,\varepsilon}|^{-1} \sum_{\mathcal{S} \in \mathbb{A}_{\eta,\varepsilon}} \mathbb{I}\{j \in \mathcal{S}\}, \quad (19)$$

which can also be generalized for two or more covariates (Kowal, 2021a). This quantity is most informative at each endpoint: $\text{VI}_{\text{incl}}(j) \approx 1$ implies that covariate j belongs to (nearly) all acceptable subsets and is therefore an essential or *keystone* covariate, while $\text{VI}_{\text{incl}}(j) \approx 0$ suggests that covariate j is irrelevant for (nearly) all acceptable subsets.

2.3 Computing the acceptable family

Computation of the acceptable family (17) has two bottlenecks: (i) exploration of the space of all subsets of $\{1, \dots, p\}$ and (ii) evaluation of the out-of-sample quantities in (14) and (16) under \mathcal{M} . To alleviate (i), we curate a collection of *candidate subsets* using a pre-screening procedure and a branch-and-bound search algorithm. The pre-screening procedure selects $s_{\max} \leq p$ covariates that have the largest effect sizes under the LMM. Although this pre-screening applies a marginal criterion, it is based on a joint model under \mathcal{M} . In that sense, this procedure is similar to the most popular Bayesian variable selection strategies based on posterior inclusion probabilities or hard-thresholding. By default, we set $s_{\max} = \min\{p, 30\}$, but note that $p > 30$ is unusual for LMMs.

Given this set of s_{\max} covariates, we apply the *branch-and-bound algorithm* (BBA; Furnival and Wilson, 2000) to filter to the “best” s_k subsets of each size $k = 1, \dots, s_{\max}$. To do so, we establish the following ordering relationship:

Lemma 2. *Let δ_1 and δ_2 denote distinct linear coefficients. Define $\hat{\Omega}^{1/2}$ such that $(\hat{\Omega}^{1/2})' \hat{\Omega}^{1/2} = \hat{\Omega}$ and let $\hat{\Omega}^{-1/2}$ be its inverse. When $\mathbb{E}_{[\tilde{\mathbf{y}}, \psi | \mathbf{y}]} \|\tilde{\mathbf{y}}(\tilde{\mathbf{X}}, \tilde{\mathbf{Z}})\|_{\hat{\Omega}_\psi}^2 < \infty$, we have the ordering equivalence*

$$\mathbb{E}_{[\tilde{\mathbf{y}}, \psi | \mathbf{y}]} \mathcal{L}\{\tilde{\mathbf{y}}(\tilde{\mathbf{X}}, \tilde{\mathbf{Z}}), \delta_1; \psi\} \leq \mathbb{E}_{[\tilde{\mathbf{y}}, \psi | \mathbf{y}]} \mathcal{L}\{\tilde{\mathbf{y}}(\tilde{\mathbf{X}}, \tilde{\mathbf{Z}}), \delta_2; \psi\}$$

if and only if

$$\|\mathbf{y}^* - \mathbf{X}^* \boldsymbol{\delta}_1\|_2^2 \leq \|\mathbf{y}^* - \mathbf{X}^* \boldsymbol{\delta}_2\|_2^2, \quad (20)$$

where $\mathbf{y}^* := \hat{\boldsymbol{\Omega}}^{-1/2} \hat{\mathbf{y}}^\Omega$ and $\mathbf{X}^* := \hat{\boldsymbol{\Omega}}^{1/2} \tilde{\mathbf{X}}$.

The proof follows similar arguments as Lemma 1 and is omitted for brevity.

Lemma 2 observes that comparisons among linear coefficients based on the expected Mahalanobis loss as in (6) can instead use the “residual sum-of-squares” (RSS) in (20) with pseudo-data \mathbf{y}^* and \mathbf{X}^* . Even though direct optimization such as (13) trivially prefers the larger of two nested subsets (as in classical subset selection), comparisons among equally-sized subsets are meaningful. BBA searches through a tree-based enumeration of all possible subsets, and avoids an exhaustive subset search by carefully eliminating non-competitive subsets (or branches) according to RSS. Hence, the RSS ordering equivalence in (20) allows us to apply BBA using the pseudo-data \mathbf{y}^* and \mathbf{X}^* and therefore obtain the “best” s_k subsets of each size $k = 1, \dots, s_{max}$. We consider the default values $s_k = 15$ or $s_k = 100$ and use the efficient BBA implementation in the `leaps` package in R. Note that computation of the pseudo-data \mathbf{y}^* and \mathbf{X}^* is a one-time cost, while the matrix square root $\hat{\boldsymbol{\Omega}}^{1/2}$ often admits fast Cholesky decompositions (e.g., block diagonality in Section 2.1.1) or direct computations (e.g., diagonality in Section 2.1.2) depending on the form of the LMM (1).

To compute the out-of-sample quantities needed for the acceptable family, we use an importance sampling algorithm. This algorithm requires only the *in-sample* posterior under the LMM and hence avoids the intensive processing of re-fitting \mathcal{M} for each of the K folds. The algorithm is detailed in the online supplement and modifies previous approaches (Kowal, 2021b; Kowal et al., 2021; Kowal, 2021a) for LMMs and Mahalanobis loss.

2.4 Predictive uncertainty quantification for each action

For any subset \mathcal{S} , we provide uncertainty quantification for the optimal linear action $\boldsymbol{\delta}_{\mathcal{S}}$ using the predictive distribution under \mathcal{M} . Specifically, we modify (6) to remove the

expectation under $p_{\mathcal{M}}\{\tilde{\mathbf{y}}(\tilde{\mathbf{X}}, \tilde{\mathbf{Z}}) \mid \mathbf{y}\}$ and therefore preserve the predictive uncertainty quantification:

$$\tilde{\boldsymbol{\delta}}_{\mathcal{S}} := \arg \min_{\boldsymbol{\delta}_{\mathcal{S}}} \mathbb{E}_{[\psi|\mathbf{y}]} \mathcal{L}\{\tilde{\mathbf{y}}(\tilde{\mathbf{X}}, \tilde{\mathbf{Z}}), \boldsymbol{\delta}_{\mathcal{S}}; \psi\} = (\tilde{\mathbf{X}}'_{\mathcal{S}} \hat{\boldsymbol{\Omega}} \tilde{\mathbf{X}}_{\mathcal{S}})^{-1} \tilde{\mathbf{X}}'_{\mathcal{S}} \hat{\boldsymbol{\Omega}} \tilde{\mathbf{y}}(\tilde{\mathbf{X}}, \tilde{\mathbf{Z}}). \quad (21)$$

This mechanism for uncertainty quantification generalizes the predictive projection approach from Kowal (2021a) to account for Mahalanobis loss. In particular, (21) includes marginalization over $\boldsymbol{\Omega}_{\psi}$ to ensure that the resulting action is exclusively a *posterior predictive* variable with a distribution induced by $p_{\mathcal{M}}\{\tilde{\mathbf{y}}(\tilde{\mathbf{X}}, \tilde{\mathbf{Z}}) \mid \mathbf{y}\}$. However, (21) can be modified to include the uncertainty of $\boldsymbol{\Omega}_{\psi}$ by replacing $\hat{\boldsymbol{\Omega}}$ with $\boldsymbol{\Omega}_{\psi}$. Posterior samples of $\tilde{\boldsymbol{\delta}}_{\mathcal{S}}$ only require posterior predictive samples of $\tilde{\mathbf{y}}(\tilde{\mathbf{X}}, \tilde{\mathbf{Z}})$ —which can be shared among all subsets \mathcal{S} of interest—and the solution to a GLS problem (21). In particular, we use (21) to compute interval estimates for the linear actions associated with \mathcal{S}_{min} and \mathcal{S}_{small} .

3 Simulation study

We evaluate the proposed LMM subset selection techniques using simulated data from a Gaussian random intercept model. First, we generate p correlated fixed effects covariates from marginal standard normal distributions with $\text{Cor}(x_{i,j}, x_{i,j'}) = (0.75)^{|j-j'|}$ for $i = 1, \dots, n$ and $j = 1, \dots, p$. The p columns are randomly permuted and augmented with an intercept. The true linear coefficients $\boldsymbol{\beta}^*$ are constructed by setting $\beta_0^* = -1$ and fixing $p_* = 5$ nonzero coefficients, with $\lceil p_*/2 \rceil$ equal to 1 and $\lfloor p_*/2 \rfloor$ equal to -1 , and the rest at zero. Let $y_i^* := \mathbf{x}'_i \boldsymbol{\beta}^*$ denote the true expectation. For a given intraclass correlation ρ_* and signal-to-noise ratio SNR, define $\sigma_{tot}^2 := \text{var}(\{y_i^*\}_{i=1}^n) / \text{SNR}$ and let $\sigma_u^2 := \rho_* \sigma_{tot}^2$ and $\sigma_{\epsilon}^2 := \sigma_{tot}^2 - \sigma_u^2$. The data are generated as $y_{ij} = y_i^* + u_i + \epsilon_{ij}$ where $u_i \stackrel{iid}{\sim} N(0, \sigma_u^2)$ and $\epsilon_{ij} \sim N(0, \sigma_{\epsilon}^2)$ for $j = 1, \dots, m_i$ and $i = 1, \dots, n$. We simulate the number of within-subject replicates $m_i = \max\{2, \text{Poisson}(5)\}$, fix $p_* = 2$ true signals (plus an intercept) and intraclass correlation

$\rho_* = 0.5$, and consider $p \in \{15, 35\}$ predictors, $n \in \{25, 50, 100\}$ subjects, and $\text{SNR} \in \{0.25, 0.7\}$ (results for $\text{SNR} = 1$ are similar to $\text{SNR} = 0.7$ and are omitted). We repeat the data-generating process 100 times for each design.

We implement a Bayesian LMM using the `rstanarm` package in R. We adopt the default priors from `stan_lmer` with horseshoe priors for β and a prior expected number of signals of $p/4$. Using \mathcal{M} , we compute the acceptable family $\mathbb{A}_{0,0.10}$ with $s_k = 15$. For each member of the acceptable family—with a special focus on \mathcal{S}_{small} and \mathcal{S}_{min} —we compute point estimates $\hat{\delta}_{\mathcal{S}}$, point predictions $\mathbf{x}'\hat{\delta}_{\mathcal{S}}$, and 90% intervals for β^* using the posterior quantiles of $\tilde{\delta}_{\mathcal{S}}$.

The primary Bayesian competitor for point and interval estimation, prediction, and selection is given by the usual actions under the Bayesian LMM \mathcal{M} . Point estimates and predictions are computed from the posterior mean $\hat{\beta}$ and $\mathbf{x}'\hat{\beta}$, respectively, and the 90% intervals for β^* are estimated using the 90% highest posterior density (HPD) intervals for β . To select fixed effects from \mathcal{M} —as a competitor to \mathcal{S}_{small} and \mathcal{S}_{min} —we adopt the common strategy of selecting variables marginally based on whether the 95% HPD intervals for each β_j exclude zero. Lastly, we compare against classical variable selection methods that do not account for the random effects. Specifically, we apply the adaptive lasso (tuning parameter selected via 10-fold cross-validation and the one-standard-error rule) and classical subset selection (using Mallows’s C_p) to the data $\{(\mathbf{x}_i, \bar{y}_i)\}_{i=1}^n$ for $\bar{y}_i := m_i^{-1} \sum_{j=1}^{m_i} y_{ij}$. 90% intervals for β^* are computed using confidence intervals from a linear regression model that includes only the variables selected by the adaptive lasso (Zhao et al., 2017). We attempted to include fence-based variable selection for LMMs (Jiang et al., 2008), but the R package `fence` failed to converge for our simulation settings with $p \geq 10$.

We compare point prediction accuracy using Mahalanobis loss for y_i^* , where the Mahalanobis weight matrix (10) uses the true parameters for σ_ϵ^2 and σ_u^2 . These results are presented in Figure 1; results for root mean squared error for y_i^* and β^* are in the online supplement. Figure 1 also summarizes the selected subset sizes; the posterior mean is dense

so its subset size is always $p + 1$. The best point predictors are consistently from \mathcal{S}_{small} and the posterior mean under \mathcal{M} . Notably, the smallest acceptable subset size $|\mathcal{S}_{small}|$ is stable and concentrated around the “true” subset size, while the competing methods are more variable and often select unnecessarily large subsets. Hence, \mathcal{S}_{small} offers substantial reductions in the subset size while maintaining (nearly) the best prediction accuracy among these methods—which is precisely the goal of the smallest acceptable subset.

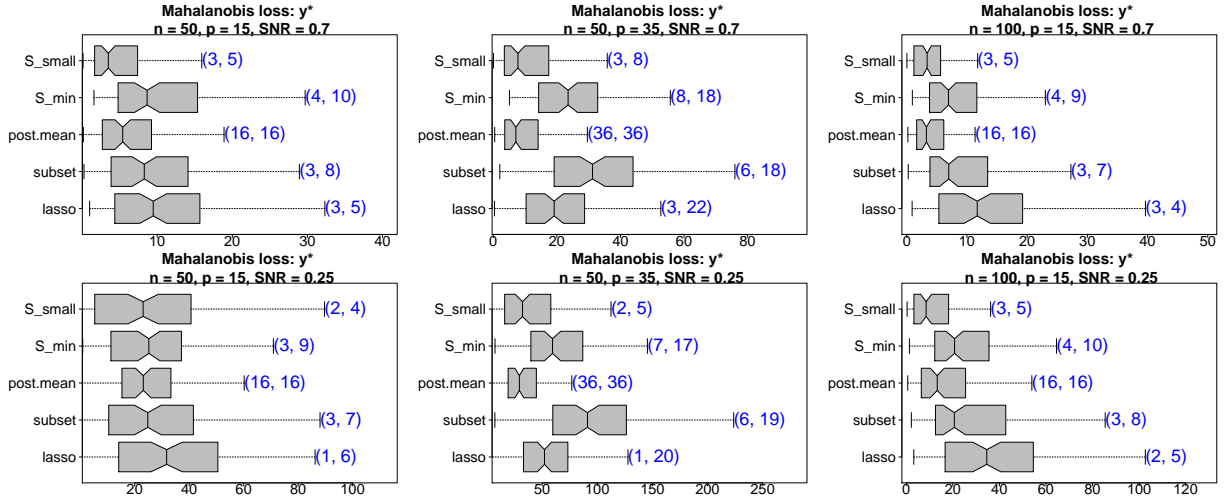


Figure 1: Mahalanobis loss for predicting y_i^* (boxplots) with 90% intervals for the subset sizes (annotations). Non-overlapping notches indicate significant differences between medians. The smallest acceptable subset offers or matches the best prediction accuracy, while $|\mathcal{S}_{small}|$ remains small and close to the true model size ($p^* + 1 = 3$).

The 90% interval estimates for β^* are evaluated in Figure 2, which reports the mean interval widths and the empirical coverage; narrow intervals that provide the correct nominal coverage are preferred. The intervals from \mathcal{S}_{small} are clearly the best in these simulation designs: the intervals maintain 90% coverage and are much narrower than competing methods. In particular, the intervals from \mathcal{S}_{small} are far more precise (i.e., narrower) than the 90% HPD intervals under \mathcal{M} . Perhaps surprisingly, the intervals from \mathcal{S}_{min} are not competitive with those from \mathcal{S}_{small} and suffer from undercoverage.

To quantify the overall predictive performance of the acceptable family $\mathbb{A}_{\eta, \varepsilon}$, we compute

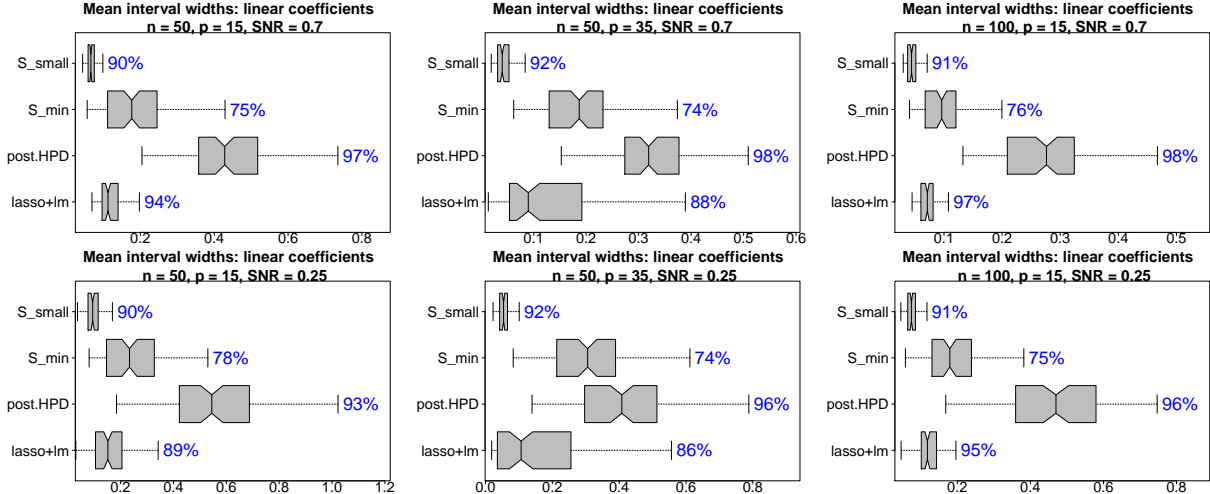


Figure 2: Mean 90% interval widths (boxplots) with empirical coverage (annotations) for β^* . Non-overlapping notches indicate significant differences between medians. The proposed intervals based on \mathcal{S}_{small} are significantly narrower than the usual HPD intervals under \mathcal{M} yet maintain the nominal 90% coverage.

the q th quantile of the true Mahalanobis loss for each acceptable subset at each simulation, and then average that quantity across simulations to obtain $\mathbb{A}^{(q)}$. For example, $\mathbb{A}^{(1)}$ is the worst possible performance in the acceptable family, i.e., if an oracle were to select the worst acceptable subset at each simulation. The results are presented in Table 1. The smallest acceptable subset is an outstanding member of the acceptable family: \mathcal{S}_{small} outperforms both \mathcal{S}_{min} and the “median” acceptable subset $\mathbb{A}^{(0.5)}$. In addition, \mathcal{S}_{small} often matches or exceeds the predictive accuracy of $\hat{\beta}$ under \mathcal{M} —despite a substantial reduction in the subset size (see Figure 1)—while the top 10% of acceptable subsets ($\mathbb{A}^{(0)}$ and $\mathbb{A}^{(0.1)}$) are highly competitive in all settings. Perhaps surprisingly, the bottom 10% of acceptable subsets ($\mathbb{A}^{(0.9)}$ and $\mathbb{A}^{(1)}$) outperform the adaptive lasso or classical subset selection as n or p increases.

Lastly, we evaluate the (marginal) variable selection capabilities using true positive rates (TPRs) and true negative rates (TNRs) in Table 2. \mathcal{S}_{small} provides consistently high TPRs and TNRs, while the 95% HPD intervals under \mathcal{M} are far too conservative for selection and suffer from extremely low TPRs. Both selection mechanisms are based on the same Bayesian

(n, p, SNR)	lasso	subset	\mathcal{M}	\mathcal{S}_{min}	\mathcal{S}_{small}	$\mathbb{A}^{(0)}$	$\mathbb{A}^{(0.1)}$	$\mathbb{A}^{(0.5)}$	$\mathbb{A}^{(0.9)}$	$\mathbb{A}^{(1)}$
(50, 15, 0.25)	33.92	30.35	24.43	27.27	26.46	13.15	18.97	27.87	35.89	43.97
(50, 15, 0.7)	12.15	10.12	6.75	10.45	6.03	4.76	6.20	9.57	11.71	13.91
(50, 35, 0.25)	53.67	96.75	33.47	66.30	39.79	23.52	41.86	61.38	71.72	77.75
(50, 35, 0.7)	21.58	32.91	10.57	24.67	12.54	9.90	14.79	22.40	26.16	28.02
(100, 15, 0.25)	39.43	27.76	17.76	25.21	15.62	10.71	15.30	23.39	31.07	38.08
(100, 15, 0.7)	14.59	9.24	4.35	8.25	4.15	3.80	5.04	7.97	9.78	10.42

Table 1: For each simulation, we compute the q th quantile of the true Mahalanobis loss for predicting y_i^* for all acceptable subsets, and then average that quantity across simulations to obtain $\mathbb{A}^{(q)}$. \mathcal{M} refers to the posterior mean under the Bayesian LMM. \mathcal{S}_{small} clearly outperforms \mathcal{S}_{min} and the “median” acceptable subset $\mathbb{A}^{(0.5)}$, which itself outperforms the adaptive lasso and classical subset selection in nearly all cases.

LMM \mathcal{M} , but \mathcal{S}_{small} is decisively better.

4 Application

We apply our subset selection analysis to physical activity (PA) data from the 2005-2006 National Health and Nutrition Examination Survey (NHANES). Intraday PA was measured on each individual using hip-worn accelerometers for one to seven days. For each participant i on day j , we focus on moderate-to-vigorous activity $MVPA_{ij}$, which is defined as the number of minutes with at least 2020 activity counts and typically corresponds to more intensive activities that include vigorous walking or running (Fishman et al., 2016). The goal is to determine the subject-specific factors that predict MVPA. However, these longitudinal data feature repeated measurements on each participant, and this within-subject dependence must be accounted for in both modeling and decision analysis.

We specifically analyze older (ages 65-80) and Hispanic (Mexican American or Other Hispanic) individuals. Fixed effects covariates include body mass index (BMI), age, gender (male or female), education level (less than high school, completed high school only, or some college and above), total cholesterol, HDL cholesterol, systolic blood pressure, smoking status (never, former, or current), drinking status (never, moderate, or heavy), and presence of diabetes. After filtering to individuals with at least one day of PA data, days with at least

10 hours of accelerometer wear time, PA measurements that were correctly “calibrated” and “reliable” as flagged by NHANES, and individuals with no mobility problems, the resulting analysis dataset has $N = 243$ measurements on $n = 61$ individuals with $p = 13$ covariates.

We model $y_{ij} = \log(\text{MVPA}_{ij} + 1)$ using a Bayesian random intercept model (see Section 2.1.1) with the same implementation as in Section 3 (using the default priors from `stan_lmer` with horseshoe priors on β and a prior expected number of signals of $p/4$); results are unchanged using t_3 priors for β . Residual plots indicated no clear violations of model assumptions, while \hat{R} suggested no lack of convergence and the effective sample sizes were sufficiently large (all above 2000).

Using the posterior and predictive samples from the Bayesian LMM, we compute and study the acceptable family $\mathbb{A}_{0,0.10}$. Since p is not large, we filter from the $2^p = 4096$ possible subsets to the “best” $s_k = 100$ models of each size $k = 1, \dots, s_{max} = p + 1$ (the intercept is always included), which produces 974 candidate subsets. Figure 3 summarizes the predictive performance among these candidates using Mahalanobis predictive loss. For instance, the intercept-only model ($|\mathcal{S}| = 1$) performs around 35% to 65% worse than \mathcal{S}_{min} , where this uncertainty derives from the predictive distribution under \mathcal{M} . The acceptable family has $|\mathbb{A}_{0,0.10}| = 141$ members ranging from sizes 4 to 9, including $|\mathcal{S}_{small}| = 4$ and $|\mathcal{S}_{min}| = 7$. Performance for both larger and smaller subsets deteriorates, although several of these subsets would be acceptable under larger margins such as $\eta = 5\%$.

To summarize the $|\mathbb{A}_{0,0.10}| = 141$ subsets within the acceptable family, we report the variable importance metric $\text{VI}_{\text{incl}}(j)$ in Figure 4. Gender, age, and total cholesterol are keystone covariates that appear in all acceptable subsets, and are the only members (plus the intercept) of \mathcal{S}_{small} . Notably, the remaining covariates appear in some—but not most—of the acceptable subsets. These covariates are not entirely extraneous, but appear to be interchangeable and not strictly necessary for acceptable linear prediction. Interestingly, the “best” subset \mathcal{S}_{min} adds smoking status (current), drinking (heavy), and diabetes to \mathcal{S}_{small} .

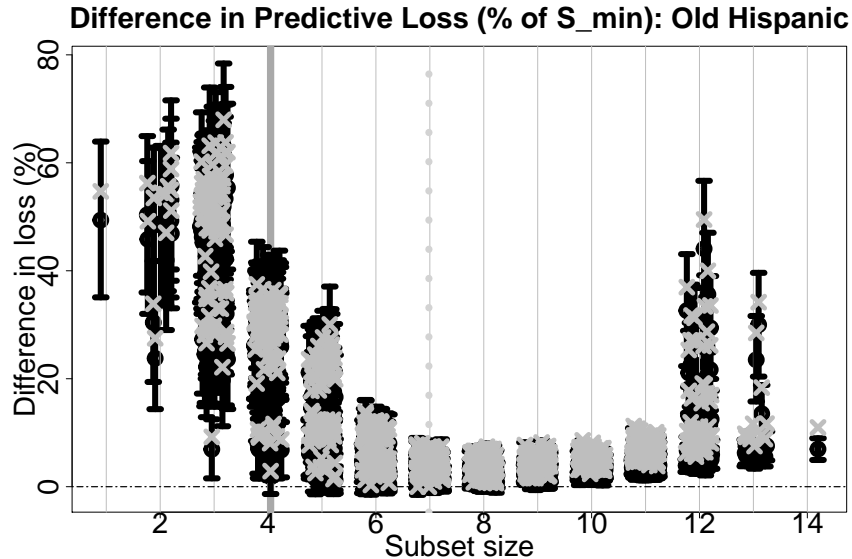


Figure 3: Prediction 80% intervals (lines) and expectations (points) for $\tilde{\mathcal{D}}_{\mathcal{S}_{min}, \mathcal{S}}$ across candidate subsets \mathcal{S} (including the intercept). The analogous empirical quantity, $\mathcal{D}_{\mathcal{S}_{min}, \mathcal{S}} := 100 \times (\mathcal{L}_{\mathcal{S}} - \mathcal{L}_{\mathcal{S}_{min}}) / \mathcal{L}_{\mathcal{S}_{min}}$, is also denoted (x-marks). Subsets of the same size are jittered for clarity of presentation. Acceptable subsets range from sizes 4 to 9, including $|\mathcal{S}_{small}| = 4$ (solid line) and $|\mathcal{S}_{min}| = 7$ (dashed line).

The variable importance provides important context for \mathcal{S}_{min} : although diabetes belongs to the “best” subset, it only appears in a small fraction (about 20%) of the acceptable subsets.

Lastly, Figure 5 compares the point and interval estimates from \mathcal{S}_{small} against the Bayesian LMM and the adaptive lasso. The methods broadly agree, and highlight a positive effect for total cholesterol—perhaps a realization of the common advice that individuals with high cholesterol should exercise more—and negative effects for gender (female) and age. \mathcal{S}_{small} produces narrower intervals among the nonzero coefficients than the HPD intervals and offers a sparsity in point estimation that is not available for the posterior means under \mathcal{M} . The frequentist intervals from Zhao et al. (2017) are difficult to interpret, since they often fail to include the (adaptive) lasso-based point estimates from which they were derived.

Note that NHANES data are collected from a complex sampling design, and hence population-level inference typically requires survey adjustments. The oversampled groups in

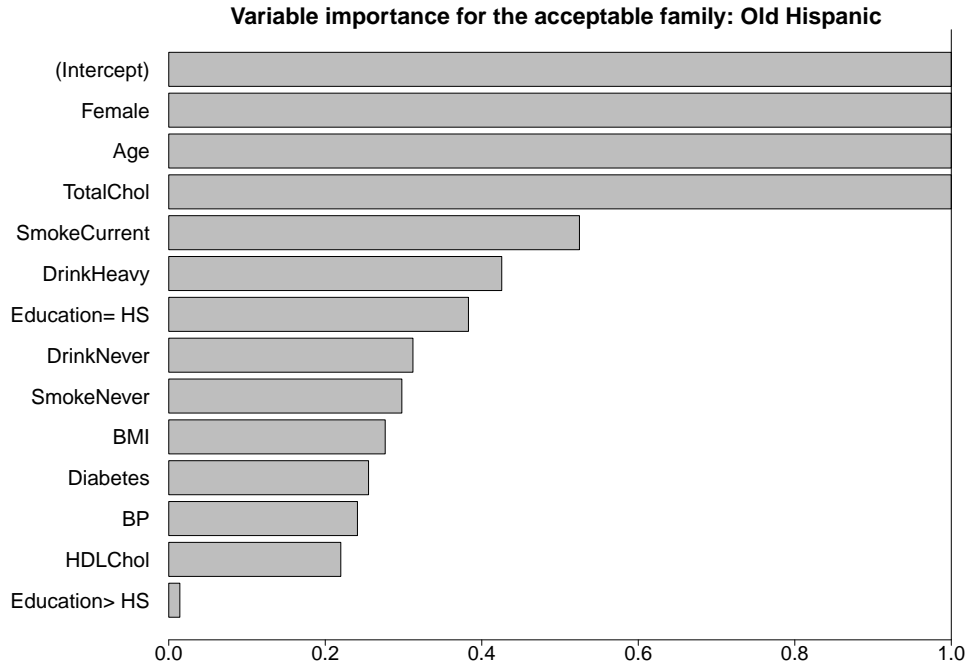


Figure 4: Variable importance $VI_{\text{incl}}(j)$ for the acceptable family $\mathbb{A}_{0,0.10}$. Gender, age, and total cholesterol are keystone covariates, while the other covariates appear in some—but not most—of the acceptable subsets.

NHANES 2005-2006 are specific age groups (12-19 and 60+ years), races (Black and Mexican Americans), and low-income individuals. Because we subset by age group and race and further include age and many other covariates in the model, we expect that the effects of the NHANES sampling design are mitigated.

5 Discussion

We have developed a decision analysis strategy for subset selection in Bayesian linear mixed models (LMMs). Using a Mahalanobis predictive loss function to bring forward the structured dependence from the LMM into the decision analysis, we derived optimal linear actions for any subset and under any Bayesian LMM. Each linear action is accompanied by predictive uncertainty quantification and regularization inherited from the underlying Bayesian LMM. Comparing across subsets, we collected and summarized the *acceptable*

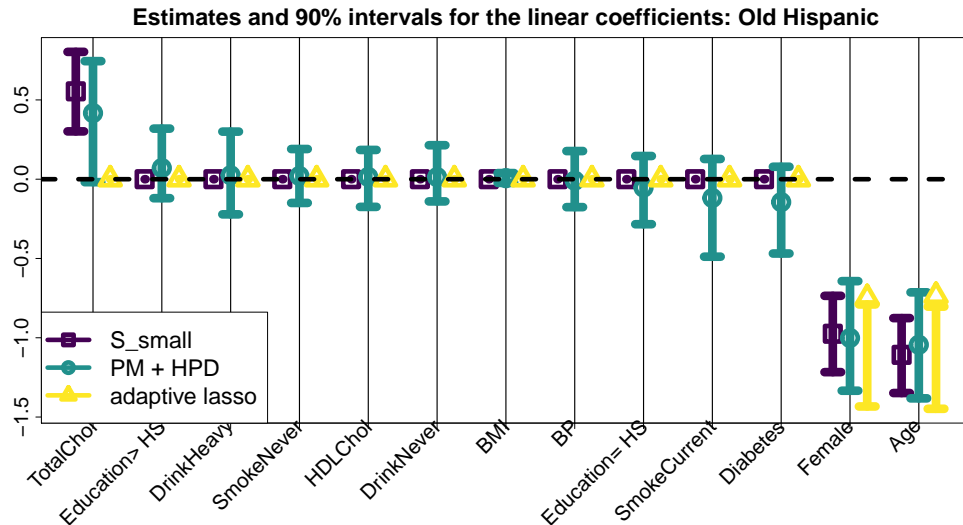


Figure 5: Estimated coefficients and 90% intervals for \mathcal{S}_{small} ($\hat{\delta}_{\mathcal{S}_{small}}$ and quantiles from $\tilde{\delta}_{\mathcal{S}_{small}}$), the Bayesian LMM \mathcal{M} (posterior means and HPD intervals for β), and the adaptive lasso (with intervals from Zhao et al., 2017). There is broad agreement, although \mathcal{S}_{small} produces narrower intervals and sparse estimates compared to the the usual Bayesian LMM estimates.

family of subsets that (nearly) matched the predictive performance of the “best” subset. The proposed tools demonstrated excellent prediction, estimation, and selection properties on simulated data, and were applied to a longitudinal dataset to study the key predictors of moderate-to-vigorous physical activity.

A primary concern with any subset selection tool is the computational cost. In fact, the computational cost of fitting the Bayesian LMM (via `stan_lmer` in `rstanarm`) dwarfed the computing costs of subset search and predictive evaluation for both the simulated and real data analyses. Our computing strategy leveraged (i) a coarse marginal pre-screening of covariates based on the Bayesian LMM, (ii) filtering to a collection of “candidate” subsets using the efficient branch-and-bound algorithm, and (iii) an out-of-sample approximation algorithm to compute the acceptable family without model re-fitting. Hence, the proposed decision analysis tools are not the limiting factor for computational scalability.

The Mahalanobis loss (4) is designed for the LMM (1), which is most commonly a Gaus-

sian LMM. However, modifications for non-Gaussian *generalized* LMMs (GLMMs) may be attainable. For Bayesian subset selection with binary data, Kowal (2021a) used iteratively-reweighted least squares (IRLS) to approximate the minimizer of a cross-entropy loss with a weighted least squares solution. IRLS is a widely popular strategy for estimating generalized linear models, and can be used to produce optimal actions under the corresponding deviance loss functions. For LMMs, a natural modification would be to insert a weighting matrix akin to Ω_ψ into the IRLS, thereby extending the proposed tools for compatibility with GLMMs.

Acknowledgements

Research was sponsored by the Army Research Office and was accomplished under Grant Number W911NF-20-1-0184. The views and conclusions contained in this document are those of the authors and should not be interpreted as representing the official policies, either expressed or implied, of the Army Research Office or the U.S. Government. The U.S. Government is authorized to reproduce and distribute reprints for Government purposes notwithstanding any copyright notation herein.

References

- Bashir, A., Carvalho, C. M., Hahn, P. R., and Jones, M. B. (2019). Post-processing posteriors over precision matrices to produce sparse graph estimates. *Bayesian Analysis*, 14(4):1075–1090.
- Bondell, H. D., Krishna, A., and Ghosh, S. K. (2010). Joint variable selection for fixed and random effects in linear mixed-effects models. *Biometrics*, 66(4):1069–1077.
- Chen, Z. and Dunson, D. B. (2003). Random effects selection in linear mixed models. *Biometrics*, 59(4):762–769.

- Fan, Y. and Li, R. (2012). Variable selection in linear mixed effects models. *Annals of statistics*, 40(4):2043.
- Fishman, E. I., Steeves, J. A., Zipunnikov, V., Koster, A., Berrigan, D., Harris, T. A., and Murphy, R. (2016). Association between Objectively Measured Physical Activity and Mortality in NHANES. *Medicine and Science in Sports and Exercise*, 48(7):1303–1311.
- Foster, S. D., Verbyla, A. P., and Pitchford, W. S. (2007). Incorporating LASSO effects into a mixed model for quantitative trait loci detection. *Journal of agricultural, biological, and environmental statistics*, 12(2):300–314.
- Furnival, G. M. and Wilson, R. W. (2000). Regressions by leaps and bounds. *Technometrics*, 42(1):69–79.
- Hahn, P. R. and Carvalho, C. M. (2015). Decoupling shrinkage and selection in bayesian linear models: A posterior summary perspective. *Journal of the American Statistical Association*, 110(509):435–448.
- Hastie, T., Tibshirani, R., and Tibshirani, R. (2020). Best Subset, Forward Stepwise or Lasso? Analysis and Recommendations Based on Extensive Comparisons. *Statistical Science*, 35(4):579–592.
- Ibrahim, J. G., Zhu, H., Garcia, R. I., and Guo, R. (2011). Fixed and random effects selection in mixed effects models. *Biometrics*, 67(2):495–503.
- Jiang, J., Rao, J. S., Gu, Z., and Nguyen, T. (2008). Fence methods for mixed model selection. *The Annals of Statistics*, 36(4):1669–1692.
- Kinney, S. K. and Dunson, D. B. (2007). Fixed and random effects selection in linear and logistic models. *Biometrics*, 63(3):690–698.

- Kowal, D. R. (2021a). Bayesian subset selection and variable importance for interpretable prediction and classification. *arXiv preprint arXiv:2104.10150*.
- Kowal, D. R. (2021b). Fast, Optimal, and Targeted Predictions using Parametrized Decision Analysis. *Journal of the American Statistical Association*.
- Kowal, D. R. and Bourgeois, D. C. (2020). Bayesian Function-on-Scalars Regression for High-Dimensional Data. *Journal of Computational and Graphical Statistics*, 29(3):1–10.
- Kowal, D. R., Bravo, M., Leong, H., Griffin, R. J., Ensor, K. B., and Miranda, M. L. (2021). Bayesian Variable Selection for Understanding Mixtures in Environmental Exposures. *Statistics in Medicine*.
- Lindley, D. V. (1968). The Choice of Variables in Multiple Regression. *Journal of the Royal Statistical Society: Series B (Methodological)*, 30(1):31–53.
- Müller, S., Scealy, J. L., and Welsh, A. H. (2013). Model selection in linear mixed models. *Statistical Science*, 28(2):135–167.
- Puelz, D., Hahn, P. R., and Carvalho, C. M. (2017). Variable selection in seemingly unrelated regressions with random predictors. *Bayesian Analysis*, 12(4):969–989.
- Wang, D., Eskridge, K. M., and Crossa, J. (2011). Identifying QTLs and epistasis in structured plant populations using adaptive mixed LASSO. *Journal of agricultural, biological, and environmental statistics*, 16(2):170–184.
- Zhao, S., Shojaie, A., and Witten, D. (2017). In defense of the indefensible: A very naive approach to high-dimensional inference. *arXiv preprint arXiv:1705.05543*.

$n = 25, p = 15, \text{SNR} = 0.25$						
	lasso	subset	posterior	HPD	\mathcal{S}_{min}	\mathcal{S}_{small}
TPR	0.53	0.63		0.22	0.74	0.55
TNR	0.90	0.79		1.00	0.68	0.94

$n = 25, p = 15, \text{SNR} = 0.7$						
	lasso	subset	posterior	HPD	\mathcal{S}_{min}	\mathcal{S}_{small}
TPR	0.84	0.88		0.35	0.91	0.83
TNR	0.85	0.82		1.00	0.64	0.95

$n = 50, p = 15, \text{SNR} = 0.25$						
	lasso	subset	posterior	HPD	\mathcal{S}_{min}	\mathcal{S}_{small}
TPR	0.71	0.86		0.34	0.89	0.77
TNR	0.94	0.84		1.00	0.77	0.97

$n = 50, p = 15, \text{SNR} = 0.7$						
	lasso	subset	posterior	HPD	\mathcal{S}_{min}	\mathcal{S}_{small}
TPR	0.97	0.98		0.74	0.97	0.97
TNR	0.95	0.85		1.00	0.73	0.97

$n = 50, p = 35, \text{SNR} = 0.25$						
	lasso	subset	posterior	HPD	\mathcal{S}_{min}	\mathcal{S}_{small}
TPR	0.65	0.70		0.31	0.80	0.70
TNR	0.86	0.71		1.00	0.71	0.96

$n = 50, p = 35, \text{SNR} = 0.7$						
	lasso	subset	posterior	HPD	\mathcal{S}_{min}	\mathcal{S}_{small}
TPR	0.89	0.90		0.59	0.93	0.92
TNR	0.85	0.71		1.00	0.70	0.95

$n = 100, p = 15, \text{SNR} = 0.25$						
	lasso	subset	posterior	HPD	\mathcal{S}_{min}	\mathcal{S}_{small}
TPR	0.94	0.98		0.63	0.99	0.95
TNR	0.97	0.83		1.00	0.74	0.97

$n = 100, p = 15, \text{SNR} = 0.7$						
	lasso	subset	posterior	HPD	\mathcal{S}_{min}	\mathcal{S}_{small}
TPR	1.00	1.00		0.99	1.00	1.00
TNR	0.99	0.84		1.00	0.77	0.97

Table 2: True positive rates (TPR) and true negative rates (TNR) for synthetic data with $p^* + 1 = 3$ active covariates including the intercept. \mathcal{S}_{small} provides consistently high TPRs and TNRs, while the 95% HPD intervals under \mathcal{M} are far too conservative (extremely low TPRs).